Winter 2017

Determination of Metabolic Change Associated with Subarachnoid Hemorrhage

Dominique Oates
djo28@zips.uakron.edu

Determination of Metabolic Change Associated with Subarachnoid Hemorrhage

Dominique J. Oates

The University of Akron, Honors College

3150:497 1/19/2018

Introduction

Subarachnoid hemorrhage (SAH) is a type of stroke that occurs after the rupture of a brain artery into the subarachnoid meningeal space. Symptoms of the stroke include hemiplegia, slurred speech, loss of motor skills, and one-sided weakness.[1] Subarachnoid hemorrhagic strokes are more fatal than other more common strokes.[2] In many cases, patients are also at risk of complications such as septicemia, headache, stroke, and hydrocephalus.[3] Additionally, SAH patients can have continued vasoconstriction, arterial narrowing, and meningitis complicating their recovery.[4]

$$Fe^{2+} + H_2O_2 \rightarrow Fe^{3+} + OH^- + OH\bullet$$

Figure 1: Fenton chemistry: radical initiation.

The release of blood into the subarachnoid space provides an opportunity for the introduction of iron-containing compounds to the cerebrospinal fluid (CSF). Highly-reactive free iron can participate in Fenton reactions, generating free radicals and ultimately reactive oxygen species (ROS) that may result in tissue damage **(Figure 1).**[5] The relative contribution of ROS production to brain injury in SAH and whether there is a compensatory up regulation of small molecule antioxidants within the CSF has been incompletely explored.

Mass-spectroscopy based (MS-based) metabolomics has been used in the past to analyze and compare small endogenous molecules.[6] Liquid chromatography mass spectrometry (LC-MS/MS) can separate, detect, and characterize biochemicals (less than 1000Da) based on their mass-to-charge ratios and retention time.[6–8] Hydrophilic interaction liquid chromatography mass spectrometry (HILC-MS) is one of the primary methods used to detect polar metabolites which includes amino acids, citric acid cycle intermediates, and other biologically important small molecules.[9] A typical workflow for the acquisition of metabolomics datasets include compound

detection by LC-MS/MS followed by bioinformatics analysis in order to determine statistically significant changes between experimental samples. In this study, we use Elements software (version 1.2.1, Proteome Software, Inc.) to preform automated identifications and statistical comparisons between metabolites detected in CSF isolated from SAH patients and normal controls.[10]

Disturbances of iron metabolism caused by bleeding may directly impact neuronal function. As in Alzheimer patients, much of the neurodegeneration is due to oxidative stress in the brain caused by the break down of hemin.[11] The same oxidative stress is present with the degradation of hematin in CSF. When hematin is degraded in the cytosol of the cell, it causes the release of Fe^{2+}which is then oxidized into Fe^{3+}. The oxidation of the iron produces the radical hydroxyl groups, which damages proteins and DNA **(Figure 1)**.[11] The disruption of these molecules result in subsequent apoptosis in neuronal cells.[12]

In this study, we also explored iron toxicity on neuroblastoma cells by using an MTT assay. The treatment of this cell line with retinoic acid induces differentiation of the cells into a primary neuronal phenotype characterized by process extension and the production of neurotransmitters.[13,14] In addition, we utilized global metabolomics to identify changes in the CSF due to SAH. We found that treatment of differentiated neuroblastomas with hematin, an oxidation product of hemoglobin, resulted in cell death in concentrations higher than 15.62 μM. Hemin and hematin are porphyrin molecules with very similar structures. In hemin, the axial ion is chloride. While, in hematin the coordinating ion is an hydroxide ion

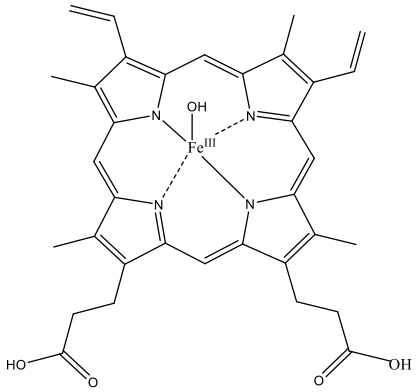

Figure 2: The structure of hematin.

(Figure 2).[15] Both iron donors contain a ferric iron at the center. The chloride ion has as higher affinity for binding oxygen than the hydroxide ion, and hemin is a primary component in the formation of hemoglobin.[16] The higher affinity for binding oxygen primes hemin for oxygen transport in blood. Hematin has a hydroxide ion that makes it a primary molecule in heme signaling.[17] Previous studies have shown that the iron coordinated in hemin altered the concentration of iron within cells. Owen et al. found that there is Fenton-chemistry occurring in the cells following the incubation of astrocytes with iron-containing hemin. They were able to measure the concentrations of Fe^{2+} and Fe^{3+}, and found that they were both present in abundance in the cytoplasm of the cell following iron treatment. The ferric ions were found in greater concentration with a hemin containing iron treatment than a non-hemin containing iron treatment. Previous studies found that the cells had a better ability to store iron in ferritin when it was introduced through a non-hemin containing iron source. [11] These studies provide a foundation to further examine metal-mediated pathology in SAH.

Methods and Materials

Cell Culture

The SH-SY5Y human neuroblastoma cell line (ATCC CLR-2266) was cultured in a 1:1 mixture of ATCC-formulated Dulbecco's Modified Eagle Medium (DMEM) and F12 medium supplemented with 10% fetal bovine serum (FBS) and 1% penicillin streptomycin. The cells were incubated at 37ºC and 5% CO_2. This is in accordance with ATCC guidelines for cell maintenance. After cells had reached 100% confluency, they were split. Media and trypsin-EDTA were warmed to 37ºC in a hot water bath. The media was removed from the T75 plates and placed in a 50mL falcon tube. 2mL of trypsin-EDTA was added to the T75 flasks. The cells were treated with trypsin-EDTA for 2 minutes followed by the addition of 3mL of tissue culture

medium. All 5 ml of solution was subsequently added to the 50mL Falcon tube. The cell solution was then centrifuged at 1000 RPM and 4ºC for 10 minutes. After the centrifuge was completed, all of the solution was removed carefully as to not disturb the pellet. The pellet was then suspended in at least 2mL of media. The cell solution was then either plated in a T75 for continued growth, or used for a 96-well plate.

Iron Treatment and Measurement of Cell Viability

Prior to treatment with iron containing compounds, cells were plated at a density of 2.6 $x10^6$ cells/well in a final volume of 100 µl and allowed to adhere for twenty-four hours. Porcine hematin (Sigma- Aldrich, St Louis, MO) was dissolved in DMSO to create a final concentration of 2 mM. This stock solution was then serially diluted to 1µM concentration solution. Cells were incubated for an additional twenty-four hours. Following the incubation, Resazurin was added to each well at 10% of the final well volume. The resazurin was left to incubate for at least two hours and then the plate was read using the SpectraMax M2 plate reader. The absorbance was measured at a reference wavelength 690nm. The absorbance at 690nm was subtracted from the absorbance at 600nm. Fluorescent emission was measured at 590nm.

For differentiating the neuroblastomas, the cells were plated in the same way as previously described. However, 1µL of retinoic acid was added to each well and allowed to incubate for twenty-four hours prior to the administration of hematin.

Metabolite Extraction of Cerebrospinal fluid

The institutional review board at the Cleveland Clinic approved the collection and use of human CSF samples. CSF samples were stored in liquid nitrogen prior to extraction. The samples were thawed at 4°C and 100µL of the CSF was collected in Eppendorf tubes. 400µL of 4X methanol was added to each of the samples to denature the CSF. Samples were then

incubated at -20°C for two hours and centrifuged at 18,000 x g at 4°C for twenty minutes. This process separates the denatured proteins from extracted metabolites. The supernatants were collected and dried in a CentriVap Concentrator (LACONCO, Kansas, MO, US) at room temperature. The dried samples were reconstituted for analysis in 200µL of 35% acetonitrile in water.[18] Samples were then analyzed using LC-MS.

HILIC-MS

Resuspended samples were analyzed on a Micro200 LC (Ekisgent, Redwood, CA, USA) coupled with a HILC column (Luna 3µ NH_2 100Å, 150mmx 1.0mm, Phenomenex Torrance, CA, USA). HILIC employs two different mobile phases of water and acetonitrile respectively. Each phase contained an addition of 5mM ammonium acetate and 5mM ammonium hydroxide (pH 8.4). Samples were subsequently analyzed with the following gradient: 0 min 98%, 0.5 min 98%, 1 min 95%, 5 min 80%, 6 min 46%, 13 min 14.7%, 17 min 0%, 17.1 min 100%, 23 min 100%.

Following separation, samples were introduced into a 5600+ Triple ToF Mass Spectrometer (SCIEX, Framingham, MA, USA). Analysis was done in both in positive and negative mode. Nitrogen (N_2) was used as the ion source nebulizer gas (GS1) at 15 psi, the heater gas (GS2) was set to 20 psi, and the curtain gas (CUR) was set to 25 psi. The accumulation time was set to 250ms for the precursor ion acquisition. The positive mode used a +5000 V ion spray voltage and a +100 V declustering potential (DP). Fragmentation data was collected using a collision energy spread (CES) of +(20-80) V under positive mode. For negative mode, data was collected using CES of -(20-80) V.

Elements for Metabolic software (version 1.2.1, Proteome Software, Inc.) was used for data analysis following HILC-MS.[19] This software identifies compounds from MS spectra using a public database. In this case, the NIST library and combined HMDB and NIST endogenous

library were used for metabolite selection.[20] Pathways were subsequently mapped using Cytoscape software.[21]

Results

The goal of these experiments was to determine metabolic alterations associated with SAH. This was achieved by using *in vitro* viability testing and LC-MS analysis. It had been previously proposed that one source of oxidative damage in the brain is the iron-mediated production of highly reactive radical iron molecules.[22] The first task was to identify the concentration iron-containing hematin becomes toxic for the neural cells. The neuroblastomas were treated with varying concentrations of porcine hematin. The difficulty came with determining the concentration of DMSO that the hematin was soluble in, but didn't result in unnecessary cell death. **Figures 4 and Figures 5** show undifferentiated and differentiated neuroblastoma cells treated with hematin concentrations dissolved in 30% DMSO in media. In total, DMSO accounted for 3% of the well volume. There was not a clear dose-response relationship with respect to hematin-induced cell death. Very low concentrations or high concentrations of hematin appeared to impair the

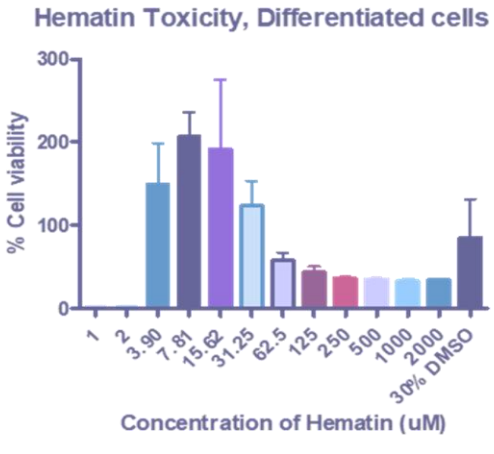

Figure 4: Differentiated SH-SY5Y treated with concentrations of hematin. Error bars represent standard deviation.

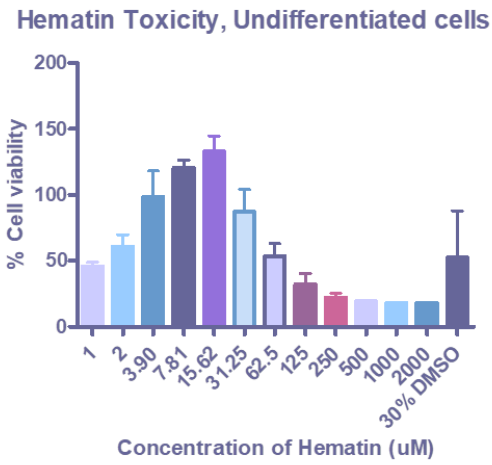

Figure 5: Undifferentiated SH-SY5Y treated with concentrations of hematin. Error bars represent standard deviation.

viability of the cells. However, at 62.5µM and above, there was a consistent loss of viability. Additionally, the vehicle had some impact on the viability of the cells. As shown in both Figure 4 and Figure 5, there was a loss of viability in cells treated only with 30% DMSO in Media. We discovered, during the differentiation protocol, that the cells needed to proliferate for a full twenty-four hours prior to being treated with the retinoic acid. This gives the neuroblastoma cells an opportunity to adhere to the plate. The standard error bars are large in the differentiated cells, because the cells were not given this time. However, in both the differentiated and undifferentiated cells, there was a significant loss in viability at 62.5µM and above.

We next analyzed CSF samples that were collected from healthy patients and patients who suffered SAH. The two sample groups were analyzed by LC-MS in order to determine metabolic changes between the two groups. Metabolite and metabolic pathway changes were explored by using Elements and Cytoscape. In Elements, metabolites that showed a fold change less than -3 and greater than 3, and that had a p-value less than or equal to 0.25 were selected as statistically significant due to the small n and the high variability in human samples.

Volcano plots showing statistically significant changes between the patients and controls are shown in **Figures 6 and 7**. The volcano plots compare the p-value s to the log fold intensities in order to determine which metabolites are significantly changed between sample groups. Positive fold changes signify an up regulation; while, negative fold changes signify a down regulation of the metabolite. Metabolites that were increased or decreased compared to controls were researched to determine their origin. Those that are endogenous were examined by using Cytoscape to map the potential pathway and enzyme interactions. For each metabolite the corresponding KEGG ID was found and used to create a network pathway in Cytoscape.

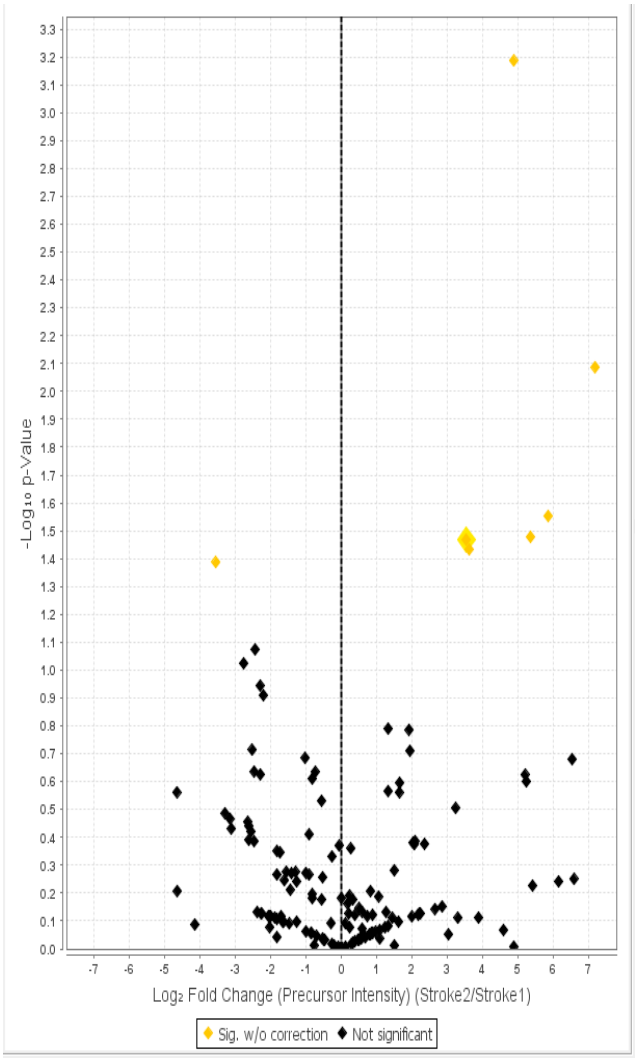

Figure 6: Volcano plot of the positive mode comparing control patients to SAH patients, made in Elements.

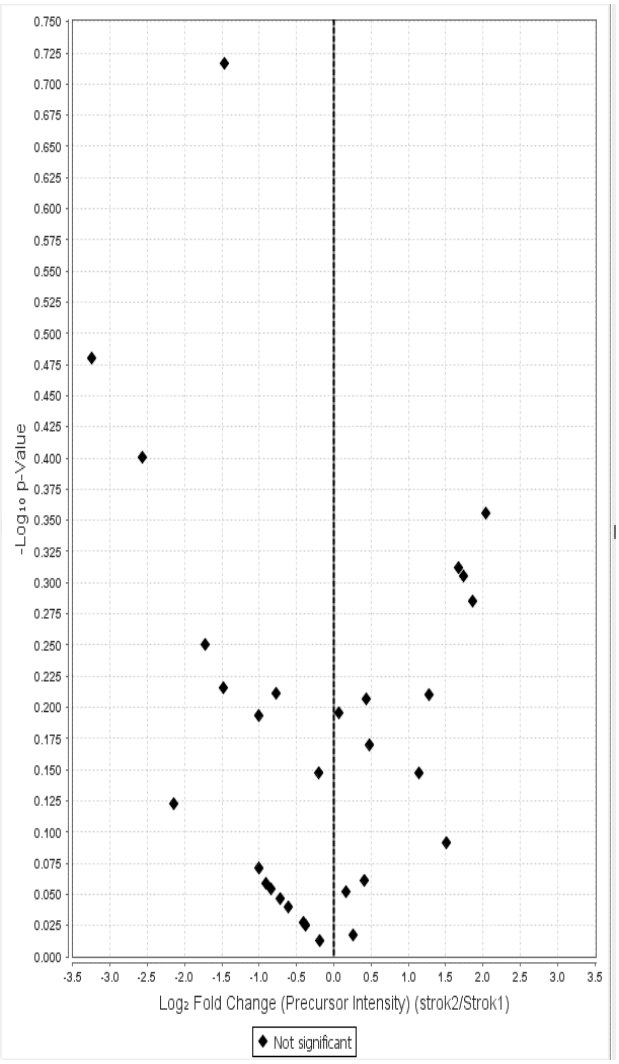

Figure 7: Volcano plot of the negative mode comparing control patients to SAH patients, made in elements.

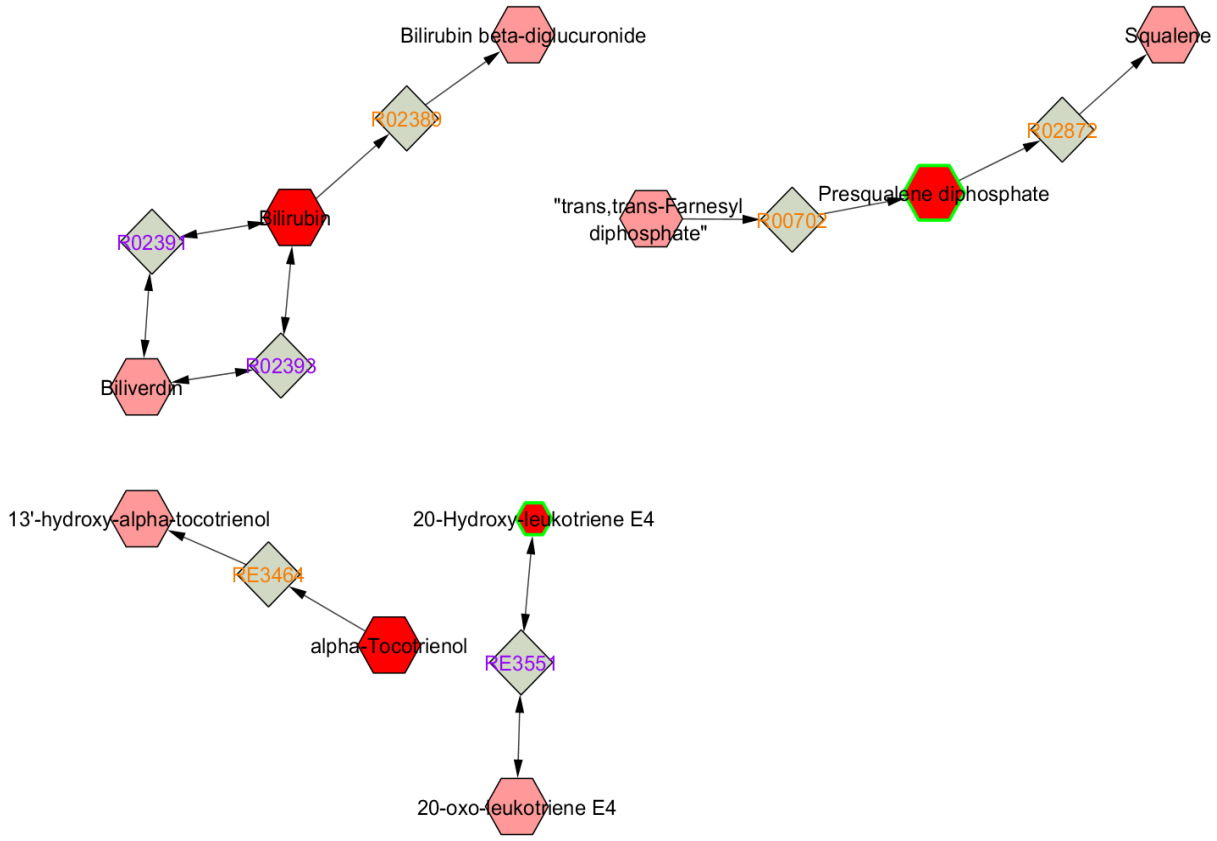

Figure 8: Pathways demonstrating significant metabolite change based on LC-MS data. Presqualene diphosphate and 20-Hydroxyl-Leukotriene E4 are both highlighted green showing significance.

Significant changes were primarily observed when metabolites were analyzed in positive mode. In patients who have suffered an SAH, there was a down regulation of 20-hydroxy-Leukotriene E4. Leukotrienes are lipid metabolites derived from arachidonic acid, an ω-6 fatty acid, and plays a role in membrane system.[23] Arachidonic acid is a major component of the cell membranes and has been detected in synaptosomes, mitochondria, and microsomes.[23] When free radicals are introduced to the cell it can trigger the peroxidation of arachidonic acid and subsequent production of pro-inflammatory lipid mediators.[24] In patients who suffered a SAH, we also saw an upregulation of adrenic acid. Many of the phospholipids in the neuronal cell membranes are comprised of arachidonic and adrenic acid. Adrenic acid is considered to be a

prothrombotic factor in the brain.[25,26] In addition, adrenic acid has been linked to neuro degeneration. A recent study demonstrated an upregulation of adrenic acid in the grey matter of Alzheimer patients when compared to control patients.[27] We also observed an upregulation of γ-glutamyl-L-putrescine. This metabolite is part of the putrescine degradation pathway and putrescine can contribute to the production of the inhibitory neurotransmitter, GABA.[28] Therefore, alterations in putrescine levels after SAH may impact the balance between inhibitory transmitters such as GABA and excitatory neurotransmitters such as glutamate. Finally, the stroke patients showed an upregulation of testosterone signaling. Testosterone is reduced to 5α-dihydrotestosterone (DHT) and estrogens by the enzyme 5α-reductase. The enzyme itself is very highly concentrated in the myelin membranes.[29]

Discussion

In this study, we showed that hematin concentrations higher than 15.62 μM induced cell death in neuronal cell line. In addition, we were able to preliminarily identify metabolic pathways associated with SAH in CSF samples. Our focus was primarily on testosterone metabolism, amino acid metabolism, and leukotriene synthesis. In the future, we would like to confirm the results from our small sample size to a larger set of patients and quantify metabolite levels with selective reaction monitoring. Additionally, we need to modify the cell culture conditions to establish the concentration of DMSO that can solubilize the hematin while effectively measuring cell death. This would allow us to link alterations in CSF with changes in neuronal function induced by iron overload.

Our focus was to determine how the reactive oxygen species produced during SAH were impacting the levels of small molecule metabolites. The LC-MS data is limited due to the time restraints of the project and the number of CSF samples. However, some promising data arose

out of this experiment. One of the pathways found to be perturbed by SAH was leukotriene synthesis. Arachidonic acid, the precursor of leukotriene synthesis is often used as an inflammatory marker in mice.[30] 20-Hydroxy-Leukotriene E4 is a lipid oxidation product of leukotriene E4 and is produced in traumatic brain injury. This may contribute to edema after trauma.[31] Adrenic acid has a very similar structure to arachidonic acid and is also a ω -6 fatty acid and also showed an increase in CSF after SAH.[32] Adrenic acid can induce arterial constriction[33] and can induce inflammation in other diseases such as non-alcoholic fatty liver disease.[34] Therefore, the upregulation of this lipid may play a role in promoting post-stroke inflammation as well as vasocontstriction associated with further injury.

Testosterone metabolism in the brain is integral to the composition of grey matter.[35] Multiple cell types, such as neurons, astrocytes and oligodendrocytes, express the capability of reducing testosterone into various metabolites.[29] Estrogens and DHT that are reduced in the brain participate in remyelinating following neurodegenerative disease such as multiple sclerosis (MS). DHT has a higher binding affinity than testosterone for brain androgen receptors and has been shown to work as a remyelinating factor in the absence of testosterone.[36] DHT was discovered to combat the inflammation and demyelination of the spinal cord as MS progresses.[36] It is possible that testosterone signaling reduction in the brain is contributing to the increased inflammation following the SAH.

γ-Glutamyl-L-putrescine upregulation indicates preturbations in polyamine metabolism, which is linked to both methylation reactions and NO synthesis.[37] It is synthesized from the ATP driven reaction between putrescine and L-glutamate.[38] Polyamines can directly influence brain function by altering the activity of ion channels, and antagonists have been shown to have

neuroprotective effects during ischemic stroke.[39] The functional outcomes of dysregulation remain to be explored during SAH.

Conclusion

A subarachnoid hemorrhage causes irreversible damage to the brain tissue. The mechanism by which the tissue is injured is not well characterized. SH-SY5Y cells were used to mimic neuronal cells and determine iron toxicity. We found that high concentrations of hematin can be toxic for neuronal cell lines. However, more research is needed to determine the precise concentration that affects cell viability. LC-MS data was obtained from SAH patients and control patients. Even with the small patient number we observe alterations in metabolism associated with SAH. The affected pathways were mapped using the Cytoscape program. This showed a change in polyamine metabolism, leukotriene level, and testosterone metabolism. The significant change in the presence of these metabolites could contribute to increased inflammation and tissue damage in the brain after SAH.

Reference

(1) Nishikawa, T.; Okamura, T.; Nakayama, H.; Miyamatsu, N.; Morimoto, A.; Toyoda, K.; Suzuki, K.; Toyota, A.; Hata, T.; Yamaguchi, T. *J.*Effects of a Public Education Campaign on the Association Between Knowledge of Early Stroke Symptoms and Intention to Call an Ambulance at Stroke Onset: The Acquisition of Stroke Knowledge (ASK) Study. *Epidemiol.* **2016**, *26* (3), 115–122.

(2) D'Souza, S. *J.* Aneurysmal Subarachnoid Hemorrhage. *Neurosurg. Anesthesiol.* **2015**, *27* (3), 222–240.

(3) Rumalla, K.; Smith, K. A.; Arnold, P. M.; Mittal, M. K. Subarachnoid Hemorrhage and Readmissions: National Rates, Causes, Risk Factors, and Outcomes in 16,001 Hospitalized Patients. World Neurosurgery 2017. DOI: 10.1016

(4) Lucke-Wold, B.; Logsdon, A.; Manoranjan, B.; Turner, R.; McConnell, E.; Vates, G.; Huber, J.; Rosen, C.; Simard, J. *Int. J. Mol. Sci.* **2016**, *17* (4), 497.

(5) Provencio, J. J. Inflammation in subarachnoid hemorrhage and delayed deterioration associated with vasospasm: a review. *Acta Neurochir. Suppl.* **2013**, *115*, 233–238.

(6) Patti, G. J.; Tautenhahn, R.; Rinehart, D.; Cho, K.; Shriver, L. P.; Manchester, M.; Nikolskiy, I.; Johnson, C. H.; Mahieu, N. G.; Siuzdak, G. *Anal. Chem.* **2013**, *85* (2), 798–804.

(7) Idle, J. R.; Gonzalez, F. J. Metabolomics. *Cell Metab.* **2007**, *6* (5), 348–351.

(8) Tolstikov, V. Metabolomics: Bridging the Gap between Pharmaceutical Development and Population Health. *Metabolites* **2016**, *6* (3), 20.

(9) Cubbon, S.; Antonio, C.; Wilson, J.; Thomas-Oates, J. Metabolomic applications of HILIC-LC-MS. *Mass Spectrom. Rev.* **2010**, *29* (5), 671–684.

(10) Ostertagová, E.; Ostertag, O. Methodology and Application of Oneway ANOVA *Am. J. Mech. Eng.* **2013**, *1* (7), 256–261.

(11) Owen, J. E.; Bishop, G. M.; Robinson, S. R. Uptake and Toxicity of Hemin and Iron in Cultured Mouse Astrocytes. *Neurochem. Res.* **2016**, *41* (1–2), 298–306.

(12) Uttara, B.; Singh, A.; Zamboni, P.; Mahajan, R. Oxidative Stress and Neurodegenerative Diseases: A Review of Upstream and Downstream Antioxidant Therapeutic Options. Current Neuropharmacology 2009, 7 (1), 65–74.

(13) Shipley, M. M.; Mangold, C. A.; Szpara, M. L. Differentiation of the SH-SY5Y Human Neuroblastoma Cell Line. Journal of Visualized Experiments 2016, No. 108. DOI 10.379/53193

(14) Agholme, L.; Lindström, T.; Kågedal, K.; Marcusson, J.; Hallbeck, M. *J.* An In Vitro Model for Neuroscience: Differentiation of SH-SY5Y Cells into Cells with Morphological and Biochemical Characteristics of Mature Neuron*s. Alzheimer's Dis.* **2010**, *20* (4), 1069–1082.

(15) Gildenhuys, J.; Roex, T. le; Egan, T. J.; de Villiers, K. A. *J.*The Single Crystal X-ray Structure of β-Hematin DMSO Solvate Grown in the Presence of Chloroquine, a β-Hematin Growth-Rate Inhibitor. *Am. Chem. Soc.* **2013**, *135* (3), 1037–1047.

(16) Eike, J. H.; Palmer, A. F. Effect of Cl- and H+ on the oxygen binding properties of glutaraldehyde-polymerized bovine hemoglobin-based blood substitutes. *Biotechnol. Prog. 20* (5), 1543–1549.

(17) Liu, Q.; Wong-Riley, M. Postnatal development of N-Methyl-d-Aspartate receptor

subunits 2A, 2B, 2C, 2D, and 3B immunoreactivity in brain stem respiratory nuclei of the rat. Neuroscience 2010, 171 (3), 637–654.

(18) Soga, T. Development and Application of Capillary Electrophoresis-Mass Spectrometry Methods to Metabolomics. Metabolomics 2005, 7–24.

(19) Elements for Metabolomic http://www.proteomesoftware.com/products/elements/metabolomics/ (accessed Dec 10, 2017).

(20) Wishart, D. S.; Knox, C.; Guo, A. C.; Eisner, R.; Young, N.; Gautam, B.; Hau, D. D.; Psychogios, N.; Dong, E.; Bouatra, S.; Mandal, R.; Sinelnikov, I.; Xia, J.; Jia, L.; Cruz, J. A.; Lim, E.; Sobsey, C. A.; Shrivastava, S.; Huang, P.; Liu, P.; Fang, L.; Peng, J.; Fradette, R.; Cheng, D.; Tzur, D.; Clements, M.; Lewis, A.; De Souza, A.; Zuniga, A.; Dawe, M.; Xiong, Y.; Clive, D.; Greiner, R.; Nazyrova, A.; Shaykhutdinov, R.; Li, L.; Vogel, H. J.; Forsythe, I. B Vitamins and the Brain: Mechanisms, Dose and Efficacy--A Review.

Nucleic Acids Res. **2009**, *37* (Database issue), D603-10.

(21) Shannon, P.; Markiel, A.; Ozier, O.; Baliga, N. S.; Wang, J. T.; Ramage, D.; Amin, N.; Schwikowski, B.; Ideker, T. Cytoscape: a software environment for integrated models of biomolecular interaction networks.

Genome Res. **2003**, *13* (11), 2498–2504.

(22) Pieniazek, A.; Gwozdzinski, K. Changes in the conformational state of hemoglobin in hemodialysed patients with chronic renal failure. *Oxid. Med. Cell. Longev.* **2015**, *2015*, 783073.

(23) Murphy, R. C.; Gijón, M. A. *Biochem. J.* **2007**, *405* (3), 379–395.

(24) Anthonymuthu, T. S.; Kenny, E. M.; Bayır, H. Therapies targeting lipid peroxidation in traumatic brain injury.*Brain Res.* **2016**, *1640* (Pt A), 57–76.

(25) Human Metabolome Database: Showing metabocard for Adrenic acid (HMDB0002226) http://www.hmdb.ca/metabolites/HMDB0002226 (accessed Jan 22, 2018).

(26) Tardy, B.; Bordet, J. C.; Berruyer, M.; Ffrench, P.; Dechavanne, M. Priming effect of adrenic acid (22:4(n-6)) on tissue factor activity expressed by thrombin-stimulated endothelial cells. *Atherosclerosis* **1992**, *95* (1), 51–58.

(27) Bailey, E. &; Lockwood, E. A.; Bailey, E.; &taylor. Lipids and Development of the Human Brain *J. Biochem* **1976**, *15* (6).

(28) Caron, P. C.; Kremzner, L. T.; Cote, L. J. GABA and its relationship to putrescine metabolism in the rat brain and pancreas. *Neurochem. Int.* **1987**, *10* (2), 219–229.

(29) Celotti, F.; Melcangi, R. C.; Negri-Cesi, P.; Poletti, A. *J.* Testosterone metabolism in brain cells and membranes *Steroid Biochem. Mol. Biol.* **1991**, *40* (4–6), 673–678.

(30) Lee, H.; Villacreses, N. E.; Rapoport, S. I.; Rosenberger, T. A. *J.* In vivo imaging detects a transient increase in brain arachidonic acid metabolism: a potential marker of neuroinflammation *Neurochem.* **2004**, *91* (4), 936–945.

(31) Schuhmann, M. U.; Mokhtarzadeh, M.; Stichtenoth, D. O.; Skardelly, M.; Klinge, P. M.; Gutzki, F. M.; Samii, M.; Brinker, T. Temporal profiles of cerebrospinal fluid leukotrienes, brain edema and inflammatory response following experimental brain injury *Neurol. Res.* **2003**, *25* (5), 481–491.

(32) Kopf, P. G.; Zhang, D. X.; Gauthier, K. M.; Nithipatikom, K.; Yi, X.-Y.; Falck, J. R.; Campbell, W. B. Adrenic acid metabolites as endogenous endothelium-derived and zona

glomerulosa-derived hyperpolarizing factors.*Hypertens. (Dallas, Tex. 1979)* **2010**, *55* (2), 547–554.

(33) Mössner, J.; Hammermann, R.; Racké, K. Concomitant Down-Regulation of L-Arginine Transport and Nitric Oxide (NO) Synthesis in Rat Alveolar Macrophages by the Polyamine Spermine. Pulmonary Pharmacology & Therapeutics 2001, 14 (4), 297–305.

(34) Horas H Nababan, S.; Nishiumi, S.; Kawano, Y.; Kobayashi, T.; Yoshida, M.; Azuma, T. Adrenic acid as an inflammation enhancer in non-alcoholic fatty liver disease *Arch. Biochem. Biophys.* **2017**, *623–624*, 64–75.

(35) Skinner, E. R.; Watt, C.; Besson, J. A. O.; Best, P. V. *Brain* **1993**, *116* (3), 717–725.

(36) Hussain, R.; Ghoumari, A. M.; Bielecki, B.; Steibel, J.; Boehm, N.; Liere, P.; Macklin, W. B.; Kumar, N.; Habert, R.; Mhaouty-Kodja, S.; Tronche, F.; Sitruk-Ware, R.; Schumacher, M.; Ghandour, M. S. *Brain* **2013**, *136* (1), 132–146.

(37) Mössner, J.; Hammermann, R.; Racké, K. *Pulm. Pharmacol. Ther.* **2001**, *14* (4), 297–305.

(38) Human Metabolome Database: Showing metabocard for Gamma-glutamyl-L-putrescine (HMDB0012230) http://www.hmdb.ca/metabolites/HMDB0012230 (accessed Jan 20, 2018).

(39) Li, J.; Doyle, K. M.; Tatlisumak, T. *Curr. Med. Chem.* **2007**, *14* (17), 1807–1813.

Acknowledgments

Great thanks are due to Dr. Shriver for giving me the opportunity to work in her lab and learn from her all that I can. I would also like to thank the other graduate students of the lab who helped me and encouraged me to continue my work with the group. I hope to apply all I have learned from this group of amazing people.

Safety Considerations

A sterile technique was utilized during cell cultures and handling of biohazardous materials. This included wearing protective eyewear, gloves, and a sterile hood any time biohazardous materials were handled. Maintaining a sterile work place also included using autoclaved items and spraying all items and hood with 70% ethanol prior to experimentation. Proper lab attire was worn including lab coat, long pants, close-toed shoes, protective eyewear, and gloves. Chemicals were disposed of in the appropriate waste containers. If there was a need for chemical disposal or a lab emergency, then UA Environmental Health and Safety was contacted and able to assist.